Spring 5-2018

Wireless Power and Data Transfer Using Inductively Resonant Coils

Seth C. Raymond
University of Maine

WIRELESS POWER AND DATA TRANSFER USING INDUCTIVELY RESONANT COILS

by

Seth C. Raymond

A Thesis Submitted in Partial Fulfillment
of the Requirements for a Degree with Honors
(Electrical Engineering)

The Honors College

University of Maine

May 2016

Advisory Committee:
Nuri Emanetoglu, Professor of Electrical and Computer Engineering, Advisor
Andrew Sheaff, Professor of Electrical and Computer Engineering
Donald Hummels, Professor of Electrical and Computer Engineering
Elizabeth Payne, Professor of English
Melissa Ladenheim, Associate Dean, Honors

Abstract

In electronics, resonance occurs when the admittances of circuit components, the imaginary parts of the component impedances, cancel each other out. Operation of circuits at their resonant frequencies can cause oscillation of signals at extreme levels. Nikola Tesla developed the concept of harnessing the capabilities of resonance by transmitting energy wirelessly between two inductively resonant coils. In 1897, his newly patented design, known as the Tesla coil, was an early prototype used to realize his theory. However, only in relatively recent history has the idea been expanded upon and used for commercial applications. Medical devices, such as pacemakers, are powered through resonant inductive coupling; this form of wireless technology has been in use since the 1960s. Battery-operated toothbrushes are typically charged with one or more small coils in the toothbrush and in the cradle, with power transmitted from the cradle to the toothbrush wirelessly. Newer emerging technology, such as radio-frequency identification (RFID) and near field communication (NFC) has provided end-users with relatively simple products for proximity dependent interaction with their personal devices, such as smartphones. This paper describes the theory and limitations of this emerging technology through the design and construction of a wireless NiCd battery charger, as well as through an investigation of some of the more common protocols for wireless data transmission.

Contents

List of Figures **iv**

1 Introduction **1**

2 Mechanics of Wireless Transmission **1**

3 Wireless Power Transfer **4**

3.1 Common Wireless Power Transmission Applications 4

3.2 Power Transmission Module 5

3.2.1 Power Transmission Design 6

3.2.2 Power Transmission Construction and Results 12

3.3 Power Receiving Module 13

3.3.1 Power Receiving Design 13

3.3.2 Power Receiving Construction and Results 17

4 Wireless Data Transmission **18**

4.1 Near Field Communication Applications 19

4.1.1 Application Data Transferal 20

4.1.2 Monetary Transactions 20

4.2 Near Field Communication Limitations 20

5 Conclusion **21**

References **22**

A Schematics **23**

List of Figures

1 Magnetic flux through Coil 2 due to current I_1 3
2 Transmit module block 6
3 Generic Wien-Bridge oscillator schematic 7
4 Tuned Wien-Bridge oscillator with amplitude stabilization 8
5 Final tuned Wien-Bridge oscillator schematic 9
6 Driver circuit schematic 10
7 Driver simulation schematic 10
8 Driver simulation results 11
9 Comparator circuit schematic with Class B amplifier output stage 12
10 Receive module block 13
11 Half-wave rectifier and voltage regulator 14
12 Simulation schematic of half-wave rectification 14
13 Unrectified EMF across simulated Rx coil 15
14 Rectified EMF across simulated Rx coil 16
15 9V NiCd battery charger 17
16 Example of phase jitter in time domain 19
17 Final transmitter schematic 23
18 Final receiver schematic 24

1 Introduction

Wireless power transmission has been in use since the 1960s, but with limited commercial applications. Due to the advances in this technology, increased consumer use has been seen in the last decade. One of the more prominent industries that is taking advantage of this form of wireless technology is the smartphone industry. Increasing numbers of smartphones and wearable technology devices are integrating wireless battery charging as well as near field communication (NFC) technology. NFC is typically used to automate simple tasks, such as turning off a phone ringer, by programming what is known as a "tag." The tag is then placed on a surface where the user will tap the phone. Once in proximity, the phone executes the programmed command. Monetary transactions can also be performed between supported devices. The intent of the addition of wireless charging and wireless data transfer is to create an easier, more intuitive user experience. The technology does, however, have its own set of limitations and restrictions. This report investigates the mechanics of wireless power transmission and gives an elementary design of a wireless NiCd battery charging system. Research on NFC uses and limitations is also presented.

Section 2 describes the electromagnetic workings of wireless transmission. Section 3 presents the design, construction, and results of a wireless battery charging system. Section 4 summarizes research on wireless data transmission used in an increasing number of smartphones. Section 5 concludes the report.

2 Mechanics of Wireless Transmission

Passive circuit components include resistors, capacitors, and inductors. Each of these components have an impedance associated with them, meaning they oppose the flow of current when a voltage is applied across the terminals of the component. Impedance can be broken up into real and imaginary parts. Ideally, resistors have purely real impedances, whereas capacitors and inductors have purely imaginary impedances. The impedances of capacitors and inductors are frequency dependent. Frequency is represented as ω in this section. Equation 1 below describes the impedance Z_L of an inductor with inductance *L*.

$$Z_L = j\omega L \tag{1}$$

Note that the impedance of an inductor will increase with frequency. This can be contrasted with the impedance of a capacitor. The impedance Z_C of a capacitor with capacitance *C* is given in Equation 2. Again, the impedance of this component is frequency dependent.

$$Z_C = \frac{1}{j\omega C} = \frac{-j}{\omega C} \tag{2}$$

Note that with capacitors, the impedance now decreases with higher frequencies. Recalling that the resonant frequency of a circuit is the frequency at which the imaginary parts of the circuit impedance is equal to zero, it can be seen that combining capacitors and inductors

in some combination will result in a resonant frequency, ω_0, based on the inductance and capacitance of the components. A particular resonant frequency, or a tuned resonant frequency, can be achieved by picking inductance and capacitance values for a given circuit topology.

An important note is that Equations 1 and 2 assume ideal components. Real world components are not ideal and include what are known as parasitic resistances, capacitances, and inductances, which will alter the given equations slightly and give rise to an error in the actual resonant frequency of the circuit. Component leads give rise to parasitic inductances. Leads and wires, such as those making up the inductive coil, produce parasitic capacitances. Finally, all wires are inherently resistive, which produces some losses. These parasitics should also be taken into account when designing resonant circuitry.

With an understanding of the concept of resonance, the physical properties of inductors can now be described. Inductors inherently oppose a change in current and do so by generating a magnetic field. This field is how the inductor stores energy. In this text, vectors are represented in bold-face. The magnetic field, **B**, at a distance *r* away from a straight wire with current *I* flowing through it is described in Equation 3. The permeability of free space, μ_0, is constant and is taken as $4\pi \times 10^{-7}[NA^{-2}]$.

$$\mathbf{B} = \frac{\mu_0 I}{2\pi r} \tag{3}$$

An inductor can be described as a wire wound about an axis. The magnetic field produced by the inductor is now focused in the direction of the axis about which the wire is wrapped. The magnetic field produced by an inductor with *N* turns and length ℓ is given in Equation 4.

$$\mathbf{B} = \frac{\mu_0 I N}{\ell} \tag{4}$$

Again, inductors can be used to store energy in a circuit. When the current through an inductor increases or decreases, the magnetic field produced by the inductor will either expand or collapse respectively. This change in magnetic field ideally keeps the number of electrons flowing through the inductor constant by either extracting energy from the inductor or returning energy to it.

The change in current also results in a change in voltage across the inductor. Through electromotive self-induction, the change in strength of a magnetic field produced by an inductor gives rise to a corresponding voltage across the inductor. This electromotive force (EMF) has a polarity that opposes the change of current. The EMF across an inductor with inductance *L* and time-changing current $\frac{dI}{dt}$ is defined in Equation 5.

$$\varepsilon = L\frac{dI}{dt} \tag{5}$$

With the knowledge of how energy is stored in an inductor, a related parameter can now be described. The magnetic flux is defined as the amount of magnetic field passing through a

given area. Magnetic flux, Φ, is mathematically defined in Equation 6.

$$\Phi = \mathbf{B} \cdot \mathbf{A} = |\mathbf{B}||\mathbf{A}|cos(\theta) \tag{6}$$

It should be noted that the vector area of the surface **A** has a magnitude equal to the surface area of the object and points normal to the surface. The value of θ is defined as the angle between **B** and **A**.

With the definition of magnetic flux, it is now possible to describe the transmission of power between the two inductors. Consider the condition shown in Figure 1, which was taken from the online MIT Electromagnetics course notes.

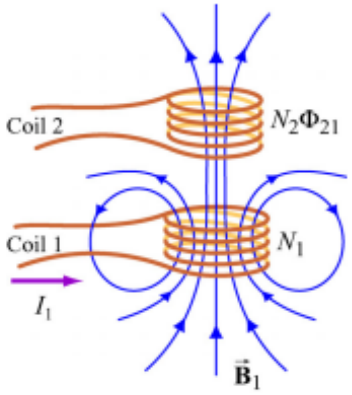

Figure 1: Magnetic flux through Coil 2 due to current I_1 [1]

Recall that the magnetic field $\mathbf{B}_1$ is produced by Coil 1 in order to store energy if current I_1 changes. Placing the coils in close proximity to one another results in the magnetic field produced by Coil 1 passing through Coil 2, giving rise to magnetic flux Φ_{21}. The EMF across Coil 2 due to Coil 1, ε_{21}, is a function of the change in magnetic flux and is given below in Equation 7.

$$\varepsilon_{21} = -N_2 \frac{d\Phi_{21}}{dt} \tag{7}$$

This property is called mutual inductance. The energy stored by Coil 1 is captured by Coil 2, which induces an electromotive force across Coil 2. However, the electromotive force across Coil 2 is only produced if the current I_1 changes. The mutual inductance proportionality constant is defined as M, where $0 < M < 1$. The mutual inductance proportionality constant between Coil 1 and Coil 2, M_{21}, can be found using Equation 8.

$$N_2 \frac{d\Phi_{21}}{dt} = M_{21} \frac{dI_1}{dt} \tag{8}$$

By substituting Equation 7 into Equation 8, it can be seen that the mutual inductance proportionality constant shows how efficiently Coil 2 transforms the magnetic field $\mathbf{B}_1$ into a usable voltage. A higher mutual inductance proportionality constant means the coils

are better physically matched, giving a higher magnitude of voltage with the same time-varying current. The value of M is dependent on the physical characteristics of the two coils, including the number of turns of the wire, the diameter of the wire that makes up the coil, and the geometry, or whether the coil windings are stacked vertically, or expand out horizontally. The coefficient is also dependent on the physical proximity of the two coils.

Plugging Equation 8 into Equation 7 shows that the voltage across Coil 2, the EMF, is dependent on how much the current through Coil 1 varies with time. A rapid change in current through Coil 1 will produce a large voltage across Coil 2. In design, it is typically desirable to have a large voltage across the inductor corresponding to Coil 2, as the voltage can be stepped down with standard circuit topologies, such as a buck converter.

3 Wireless Power Transfer

By using the mechanics outlined in Section 2, hardware can be designed to cause a "transmission coil" to produce a magnetic field. A "receiving coil" placed in this magnetic field can harness the transmitted energy and transform it into a usable voltage. These coils correspond to Coil 1 and Coil 2 in the previous section, respectively. This transmission typically occurs over relatively short distances. Recall that the amount of current produced in the receiving coil is related to the proportionality constant M. The value of M is highly dependent on distance, and a larger distance results in a significantly smaller value. The AC voltage signal induced across the receiving coil is often rectified into a DC voltage source.

Section 3.1 describes some of the common applications for wireless power transmission. Section 3.2 introduces the power transmission source and is further broken down into the design, construction, and testing of the source. Section 3.3 similarly introduces the power receiving circuitry, and is broken down into the design, construction, and testing of a 9V NiCd battery charging circuit.

3.1 Common Wireless Power Transmission Applications

The mutual inductance proportionality constant, defined as M in Section 2, serves to show that there are physical limitations to wireless power transmission. One of the most significant limitations is that the power receiving device needs to be in close proximity to the transmission source for good inductive coupling and increased transmission efficiency. For this reason, it does not make sense for a device to be powered solely from the EMF produced by the receiving coil. Instead, many systems that use wireless power transmission instead use it to charge a battery, which then powers the receiving side.

Many of the modern applications of wireless power transmission follow the Qi standard (pronounced "chee"). In the field of smartphone and wearable technology, many third-party manufacturers develop wireless power charging pads. These pads act as Coil 1, the transmission coil, in the scenario presented in Section 2. If these pads meet Qi specifications, they can be used to charge Qi-compliant receiving devices.

In order to be compatible, devices need to meet power efficiency specifications. These specifications are highly dependent on the mutual inductance proportionality constant between the transmission and receiving coils in the two devices. The Qi standard defines the physical properties of both coils, attempting to maximize the inductive matching. These properties include, but are not limited to, the diameter of the wire used to make the coils, the thickness of the coils, inner and outer diameters of the coils, number of layers of wire in the coils, and the number of turns per layer.

Qi recommends particular designs for coil alignment in the power transmission source, which is also referred to as a "base station" [2]. These designs include coil arrays, guided magnetic coil positioning, and free moving coils. A typical base station is in the form of a mat, with coils inside taking one of the three coil alignment designs. The mat transforms power from AC mains and produces a magnetic field compliant with the Qi standard. A device that follows the Qi wireless power receiving standard can be placed on the mat and will receive the transmitted energy.

Qi compliant base stations also typically contain some sort of a microcontroller to start and stop transmission if a receiving device is not detected, or if the receiving device no longer requires transmitted power; i.e., the battery of the device is fully charged. According to the Qi Version 1.1.2 Standard [3], communication between the receiver and transmitter is done using backscatter modulation, referring to the reflection of waves from the receiver back to the transmitter.

Modulation of a signal means particular aspects of a periodic waveform, known as a carrier signal, are adjusted. A form of modulation, called backscatter modulation, is performed on the receiving end per the Qi communication protocol. Circuitry is designed to modulate the carrier signal based on this protocol and reflect the modulated signal back to the transmitter. The transmitter detects the modulation in the returned signal and adjusts its output magnetic field according to the message received.

The transmitter parses, or interprets, the packets sent by the receiver and alters the amount of current passing through the transmission coil. If no reply is received, then the transmitter weakens the magnetic field and decreases the amount of energy transferred. This low energy state reduces the amount of electricity consumed by the transmitter as a consumer cost-saving benefit. A more in-depth analysis of the protocol is presented in Section 4.

As an Electrical Engineering capstone project, a wireless battery charging system was designed and constructed. Due to the time constraints on the project, it was not feasible to incorporate all specifications required by the Qi standard into the project. To follow the Qi standard, a communication link between the transmitter and receiver would need to be established, and circuitry to vary the magnetic field based on the data transmitted would be required.

3.2 Power Transmission Module

The first module designed for the wireless power transmission system is the Transmit module. This module takes power from AC mains and produces a magnetic field. The Transmit

module block is shown below in Figure 2.

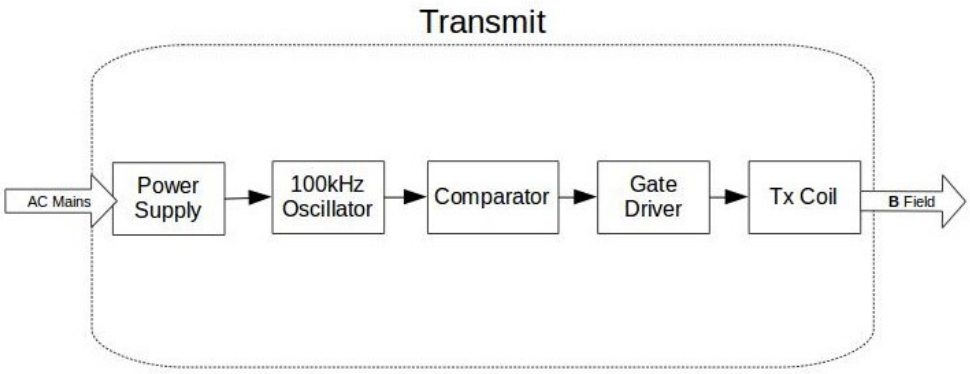

Figure 2: Transmit module block

The module input to this block is AC mains. This input is fed into the power supply, which provides $\pm$15V to the designed circuitry. An oscillator circuit creates a sinusoid, which is converted to a square wave using an op amp acting as a comparator. The square wave drives the gate of a power MOSFET, which pulses current through an inductor, denoted as the Tx coil in Figure 2. This inductor is aligned with a second, matched inductor, labeled as the Rx coil in Section 3.3.

The two matched inductors are respectively analogous to Coil 1 and Coil 2 from Section 2. These inductors ideally act as an air-core 1:1 transformer, as the matching coefficient M approaches 1. This corresponds to all of the energy in the magnetic field to be captured by the receiving coil, resulting in a perfectly mirrored voltage and current between the transmission and receiving coils. Since M is not the ideal value of 1, losses in the transmission are noticed. The Transmit module output can be described as transmitted energy that needs to be captured by the Receive module and manipulated into a usable electrical signal.

3.2.1 Power Transmission Design

The Transmit module consists of pre-fabricated power supply, an oscillator circuit, a comparator, and a gate driver circuit. A Nemic Lambda ET-4A power supply was chosen. The supply was chosen based on its ability to produce both +15V and -15V outputs, which allowed for a large peak-to-peak voltage signal oscillator output. This design choice was originally driven by the desire to operate the system in a continuous waveform mode, meaning that the signal passed through the inductor is a pure sinusoid. However, through design and testing, it was found that not enough power was being transmitted. The mode of operation was switched to a pulsed current mode of operation, which will be described later in this section. This mode of operation results in a significantly larger change in current, which induces a much larger voltage across the receiving coil, as described in Equation 5.

The op amp for the oscillator circuit was chosen to take advantage of the large supply voltages, but also needed to produce a sinusoidal signal at 100kHz, the self-resonant frequency of the transmission inductor used, an AWCCA 53N53 inductor purchased from

Digi-Key. No capacitors were used to create a resonant frequency. Instead, the parasitic capacitances of the inductors and the solderboards on which the circuitry was constructed was used to determine the self-resonant frequency. These parasitics were found in the inductor datasheet. An LF351 op amp was chosen based on the range of supply voltages allowed and the capabilities of outputting signals well above the desired oscillation frequency.

The oscillator design chosen was a Wien-Bridge oscillator circuit. The generic Wien-Bridge oscillator is shown below in Figure 3. The schematic was taken from Microelectronic Circuits 6th Edition by Sedra and Smith.

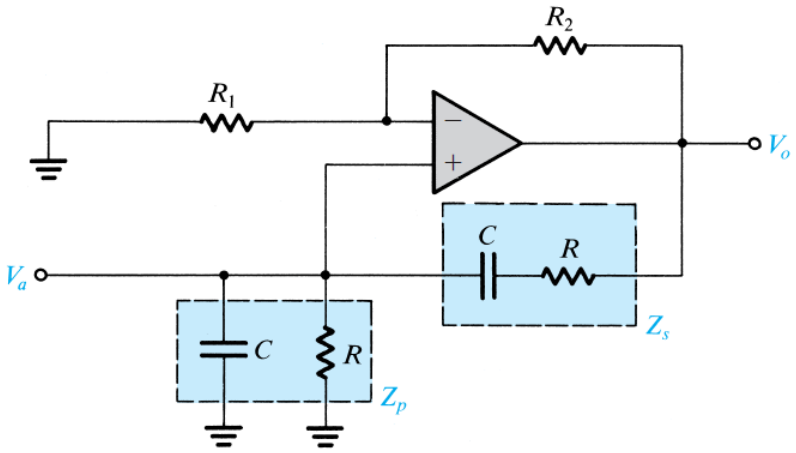

Figure 3: Generic Wien-Bridge oscillator schematic [4]

This oscillator works at a frequency of ω_0 = *1/CR* when the loop gain is approximately unity, or R_2/R_1 = 2. However, this circuit did not meet all requirements for the oscillator needed for the project. The oscillator in Figure 3 takes an input signal, V_a, which is not available in the project. As such, a similar design that excludes the input signal V_a is considered. A different variation of the generic Wien-Bridge oscillator circuit was used and is shown in Figure 4. This schematic is again taken from Microelectronic Circuits 6th Edition.

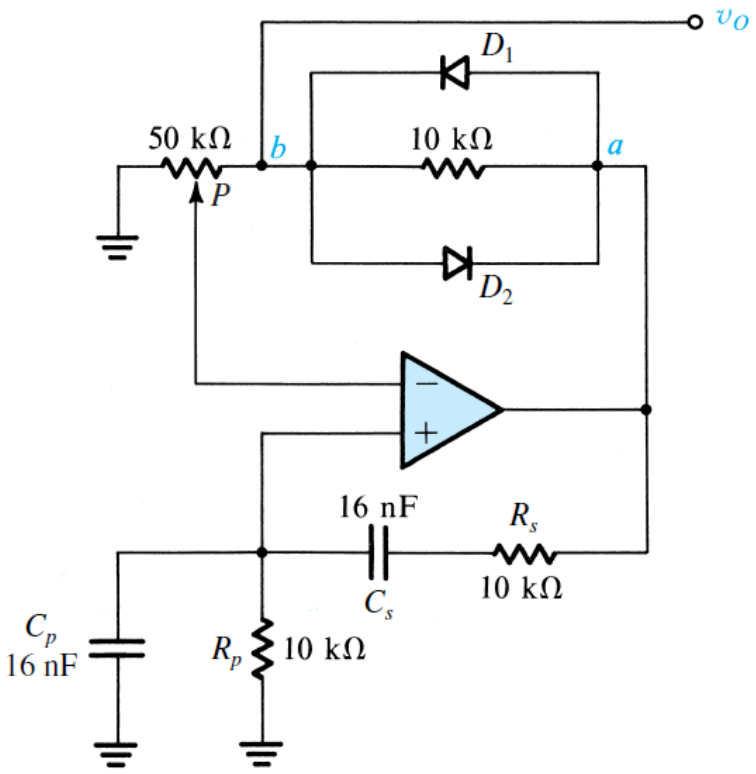

Figure 4: Tuned Wien-Bridge oscillator with amplitude stabilization [4]

By adjusting component values, the oscillation frequency can be tuned to a particular frequency. The oscillator shown in Figure 4 above is tuned for an oscillation frequency of approximately 6.3kHz. The operation of this oscillator is similar to the operation of the generic Wien-Bridge oscillator described above, but with a few distinct differences. The major difference is that the oscillator with amplitude stabilization has no input signal, and instead is initially triggered into oscillation by noise from the power supply. A handful of equations characterize the behavior of the oscillator from Figure 4. Equations 9 and 10 below give a general characterization for the parallel and series resistances and capacitances.

$$R = R_p = R_s, \tag{9}$$

$$C = C_p = C_s \tag{10}$$

Choosing values for R and C defined above determine the frequency of oscillation for the Wien-Bridge oscillator, which is shown in Equation 11 below.

$$\omega_0 = \frac{1}{RC} \tag{11}$$

It should be noted that the oscillation frequency is dependent on the network connected to the non-inverting input and the output signal amplitude is dependent on the network connected to the inverting input. The positive feedback of the oscillator has approximately zero phase shift at the resonant frequency. Therefore, both the inverting and non-inverting

inputs are approximately equal and in-phase at the resonant frequency, causing oscillation at that frequency. The potentiometer, *P*, is adjusted such that the diodes D_1 and D_2 conduct, causing the resistor between nodes *a* and *b* to be negligible. Further tuning of the potentiometer increases or decreases the amplitude of the sinusoid at the output. The two diodes also limit the gain of the oscillator such that the system does not become unstable.

It should also be noted that there is no input signal to the oscillator, which is desirable for the project. Instead, the system takes advantage of the inherent noise found in many power supplies. Since oscillators are unstable systems, the small ripple in supply voltage is amplified, triggering the oscillation at the desired frequency.

Resistance values of 1.5kΩ and capacitance values of 1nF were chosen to reach a 100kHz oscillation frequency. Like in Figure 4, a potentiometer was used to tune the amplitude of the signal. Schottky diodes were chosen over standard diodes for their low forward voltage drop. The oscillator schematic designed using Digi-Key's SchemeIt software is shown below in Figure 5.

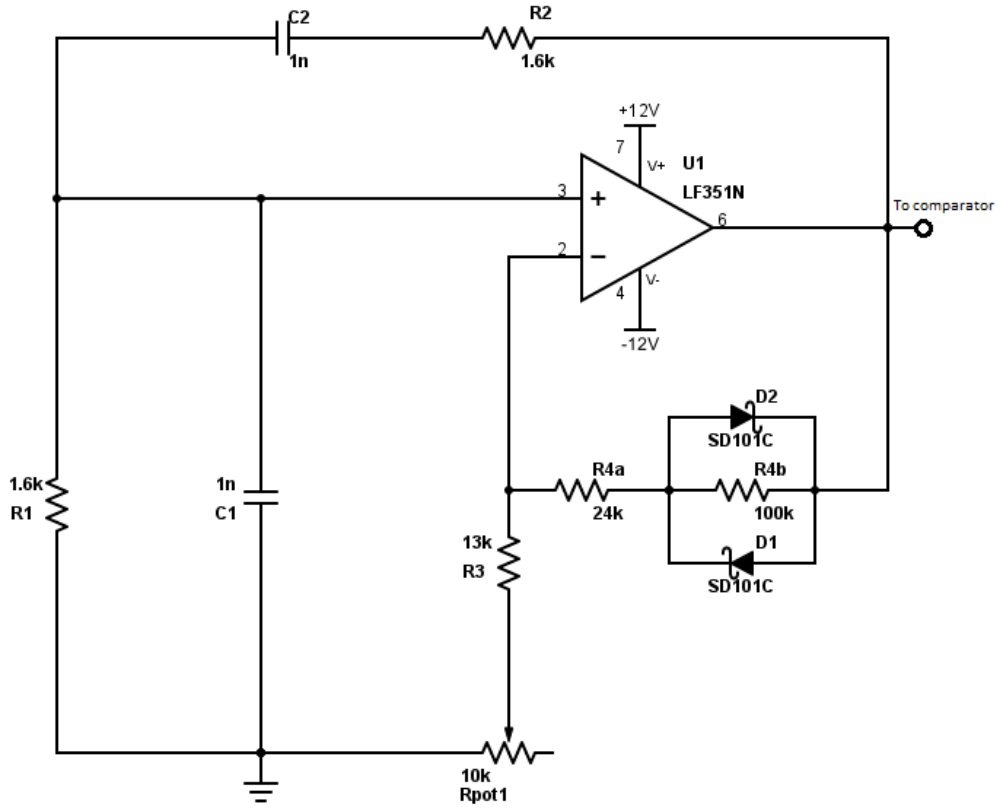

Figure 5: Final tuned Wien-Bridge oscillator schematic

The oscillator was constructed and produced the desired sinusoidal signal. However, the oscillator was incapable of driving the Tx coil, as the output impedance of the oscillator is less than the impedance of the inductor. Therefore, more circuitry needed to be designed. The chosen inductors were AWCCA 53N53 inductors purchased from Digi-Key. These inductors were chosen based on their range of operation frequencies, as well as due to the

familiarity with the product. The inductors have a nominal inductance of 24μH. To drive the Tx coil, a power MOSFET was used to pulse current through the inductor. The driver circuit, designed using Digi-Key's SchemeIt software, is shown in Figure 6. The circuit simulated in Micro-Cap Version 11 is shown in Figure 7.

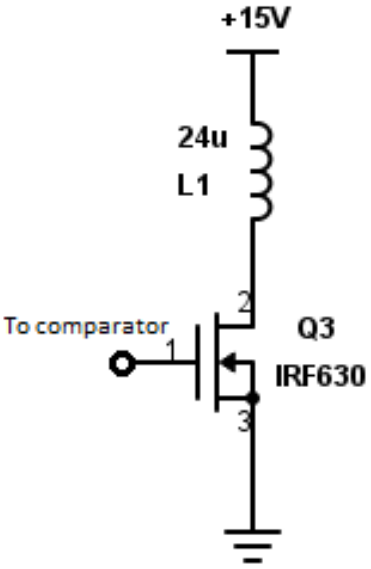

Figure 6: Driver circuit schematic

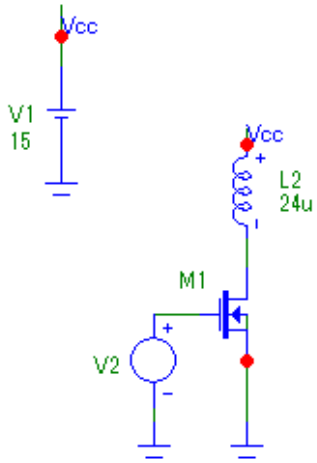

Figure 7: Driver simulation schematic

The input to the gate driver was not connected to the oscillator in the final circuit, but instead to the comparator, which will be described shortly. When the MOSFET switches on, current from the power supply is pulled through the inductor and the MOSFET to ground. When the MOSFET switches off, no current flows through the inductor, causing the necessary change in current to produce the magnetic field. The MOSFET chosen was an IRF630 power MOSFET. This MOSFET was chosen due to its high drain current ratings of up to 5.7A continuous, and due to its availability through the ECE Department.

The MOSFET M_1 is simulated as an IRF630 and the inductor L_1 is simulated as the 24μH given in the datasheet for the wireless coil. The body effect of the transistor was ignored, as the body is tied to the source of the transistor. The voltage source V_2 was simulated as a 100kHz sinusoid with a 12V peak voltage. A transient simulation was run using Micro-Cap, and the results of the simulation are shown below in Figure 8. The data was extracted from Micro-Cap and plotted using MATLAB.

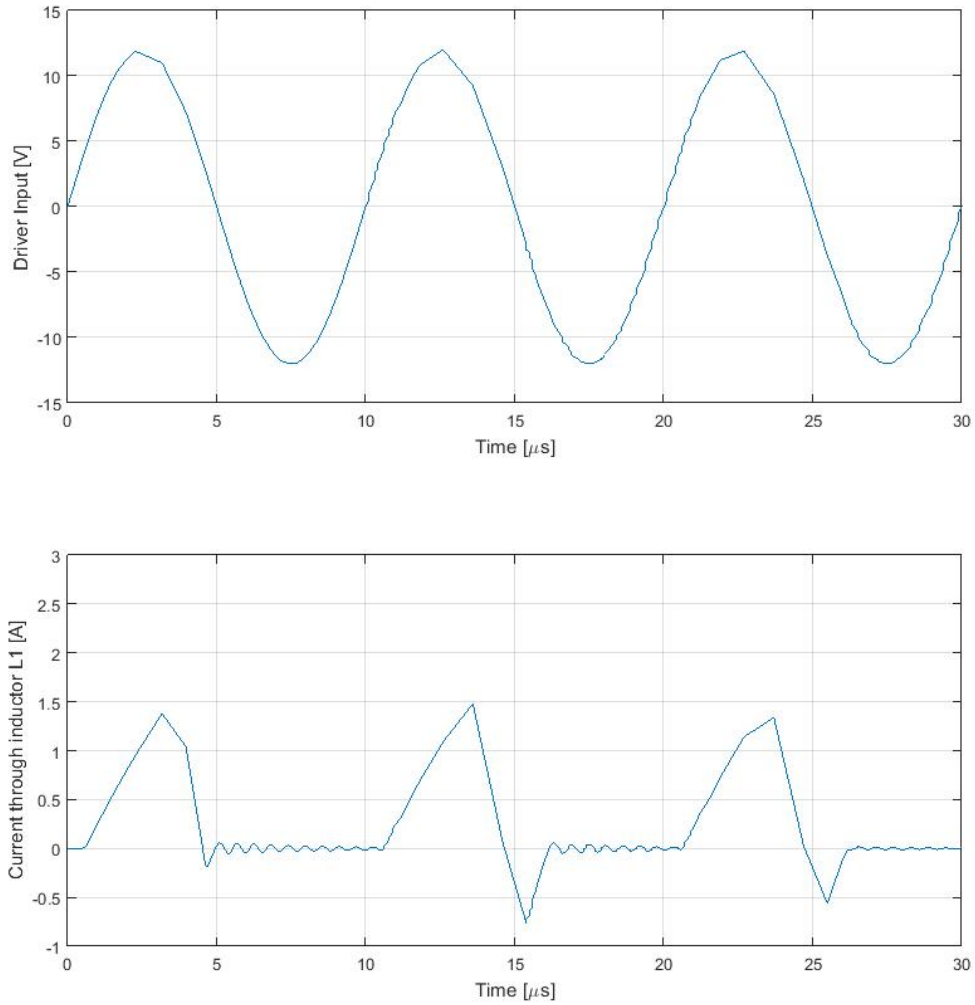

Figure 8: Driver simulation results

The top graph shows the oscillatory input to the gate of the MOSFET and the bottom graph shows the current through the inductor. The peak current through the inductor is approximately 1.5A, which is well within the safe operating range of the MOSFET.

Again, the gate of the MOSFET was originally connected to the output of the oscillator. However, through experimentation it was found that a sinusoidal input signal was not strong enough to turn the MOSFET on fully, even with a 3V V_t. By instead driving the gate of the MOSFET with a low duty cycle square wave, the MOSFET is quickly switched on fully, then switched off. This rapid change in current through the Tx coil produces a large voltage across the Rx coil, as described in Section 2.

To produce a square wave at the desired frequency, a comparator was used. An LF351 was used in a comparator circuit configuration due to its availability in the ECE Parts Store. The comparator circuit is shown in Figure 9. This schematic was also designed in the Digi-Key

SchemeIt software.

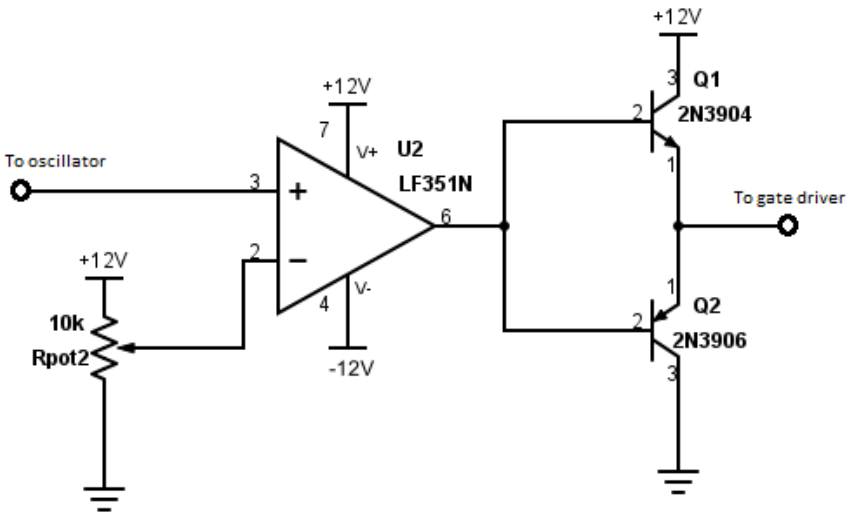

Figure 9: Comparator circuit schematic with Class B amplifier output stage

The non-inverting input to the op amp is the sinusoidal output of the oscillator. Adjusting the value of R_{pot} either increases or decreases the duty cycle. When the non-inverting input, the sinusoid produced by the oscillator, is greater than the reference voltage set by the potentiometer, the output is +12V. When the non-inverting input is less than the reference voltage, the output is -12V. The output is then passed through a Class B output stage, which acts as a voltage buffer as well as a level shifter from $\pm$12V to +12V and 0V. The reason for a voltage buffer is to transition an output signal from a high impedance source to the input of a low impedance circuit. Even though the LF351 has a high output impedance and the signal it generates is used to drive the gate of an IRF630 MOSFET, which has a low input impedance, the buffer prevents the MOSFET from loading the comparator. The Class B output stage was designed using a 2N3904 NPN BJT and a 2N3906 PNP BJT. The entire transmitter schematic, including the oscillator, comparator with output stage, and MOSFET driver circuit, can be seen in Appendix A.

3.2.2 Power Transmission Construction and Results

When constructed and tested using a CS13003x III DC Regulated power supply, it was found that the current drawn from the supply was approximately 1.1A.

Originally, the inductor was to be driven by the sinusoidal output of the oscillator. As described in the Design section, the op amp was not able to drive the low impedance of the inductor without causing loading problems. For this reason, the Class B amplifier output stage was included. It was then discovered, through experimentation, that the sinusoidal signal through the inductor did not produce a strong enough magnetic field, which led to a small current induced through the Rx coil. These results led to the inclusion of the gate driver circuit to pulse high amounts of current through the inductor.

The Wien-Bridge oscillator constructed operates at approximately 98.7kHz. The discrep-

ancy between the designed oscillation frequency and the measured frequency can be attributed to multiple issues. The design assumes that the series and parallel resistances and capacitances are exactly equal. This was not the case in the physical construction of the circuit, due to component tolerances and parasitics in the solderboard.

When testing the circuit using a CS13003x III lab power supply, the maximum current drawn from the supply through the inductor was approximately 840mA. It is assumed that the current drawn from the Nemic power supply is the same.

3.3 Power Receiving Module

The overall purpose of the Receive module is to take the energy sent from the Transmit module and transform it into a current to charge the battery. The Receive module is shown below in Figure 10.

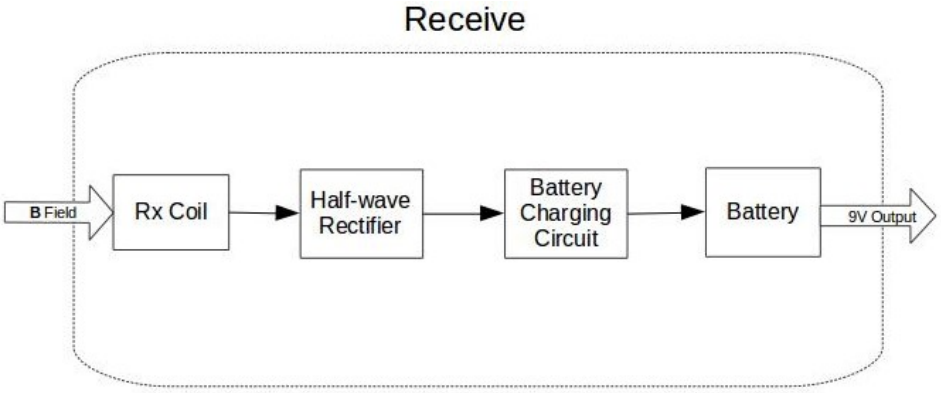

Figure 10: Receive module block

The module input for the Receive block is the module output of the Transmit block. The energy output of the Tx coil, which is a magnetic field, is seen by the Rx coil. This magnetic field induces a current through the Rx coil, which can be measured as a voltage across the inductor using Equation 5. The voltage across the Rx coil is rectified in order to power a battery charging circuit. The fully charged battery acts as the module output for the Receive block.

3.3.1 Power Receiving Design

The goal of the Receive module is to take the current induced by the Rx coil and produce a power supply for the battery charging circuit. The parameters for the battery charging circuit are dependent on several factors, including the voltage and chemistry of the battery. A 9V nickel cadmium (NiCd) battery was chosen due to the relative simplicity of the charging circuit for that chemistry.

First, the AC signal from the Receive coil is rectified and regulated. This circuitry was designed in Digi-Key's SchemeIt software and is shown below in Figure 11.

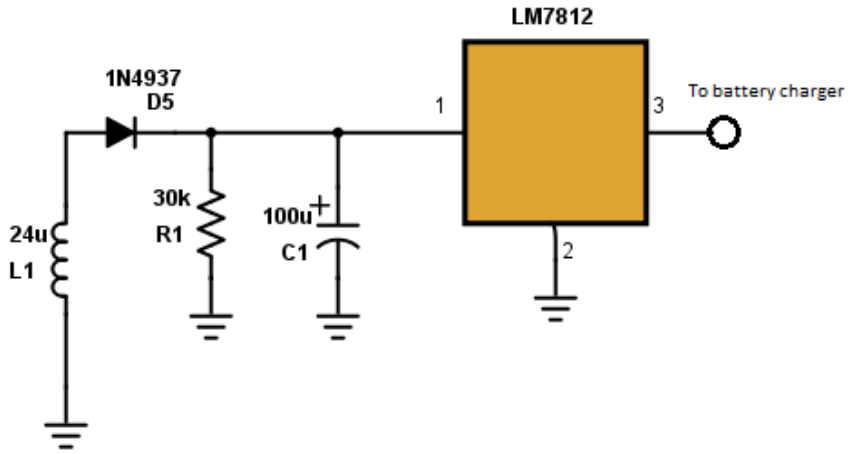

Figure 11: Half-wave rectifier and voltage regulator

Inductor L_1 from Figure 11 represents the Rx coil shown in the Receive block diagram. The EMF induced across the Rx coil is approximately equal to the voltage measured across the Tx coil, as defined in Equation 5. The current through the Rx coil is dependent on the mutual inductance coupling coefficient. In order for the signal to be capable of powering the battery charging circuitry, the signal needs to be rectified. Diode D_5, resistor R_1, and capacitor C_1 from Figure 11 creates a half-wave rectifier. A simulation schematic of the half-wave rectification circuitry is shown below in Figure 12. Simulations were again performed in Micro-Cap Version 11.

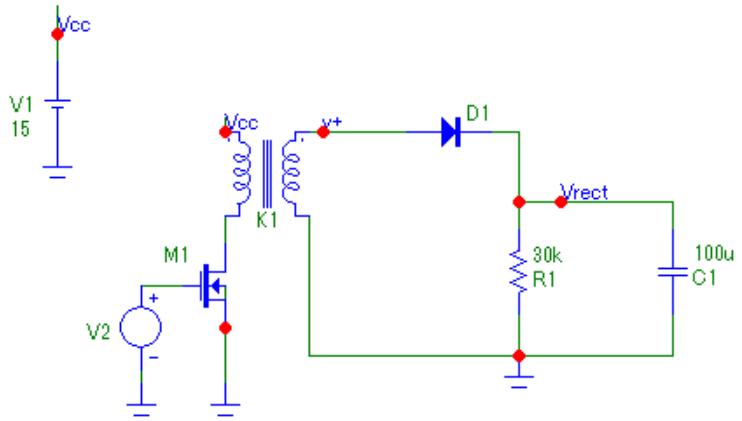

Figure 12: Simulation schematic of half-wave rectification

Transformer K_1 was simulated with both inductors having inductance 24μH as specified in the AWCCA 53N53 datasheet. The coupling coefficient was estimated to be approximately 0.8. This value was chosen based on an experiment performed where a function generator drove the Tx coil with a 5V 100kHz sinusoid. The voltage across the Rx coil was measured using an oscilloscope. The transmission efficiency with the two coils flat against each other was calculated to be approximately 80%, which gives rise to a coupling coefficient of 0.8. Voltage source V_2 is the square wave output of the Class B amplifier stage described in Section 3.2.1. Figure 13 zooms in on the EMF signal across the Rx coil before signal rectification. The data extracted from Micro-Cap was again plotted using MATLAB.

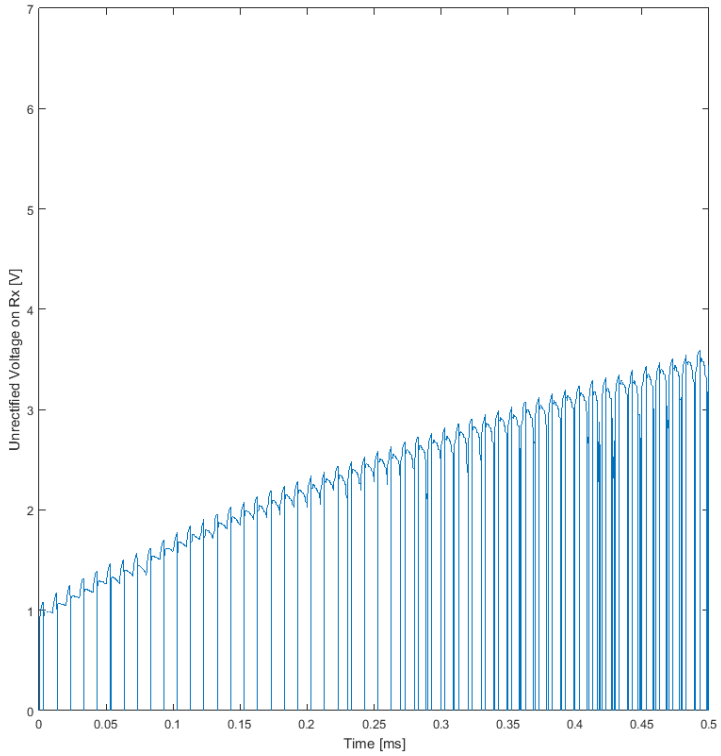

Figure 13: Unrectified EMF across simulated Rx coil

The signal is oscillatory about 0V, which is undesirable. By passing the signal through diode D_1 from Figure 12, only the positive signal remains. This resultant signal is passed through the passive RC filter created by R_1 and C_1, which smooths the signal. The maximum voltage across the Rx coil is approximately 15V. At time t=∞, the voltage at the output of the half-wave rectifier is approximately 15V. However, the rectifier output approximates the maximum 15V output in approximately 5τ seconds, which is defined as

$$\tau = RC. \tag{12}$$

By plugging in the simulated values of R and C, the rectified signal reaches a maximum at approximately 15 seconds. This scenario, however, assumes a coupling coefficient of 1. With a coupling coefficient of 0.8, the rectifier output will reach approximately 12V in 15 seconds. The rectified EMF signal is shown in Figure 14.

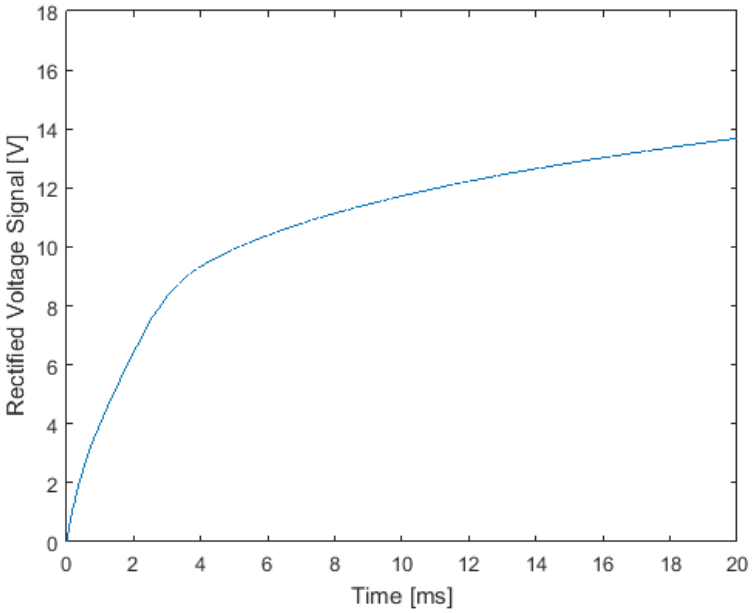

Figure 14: Rectified EMF across simulated Rx coil

Once rectified, the signal is passed through an LF7812 +12V linear drop-out voltage regulator. This produces a relatively stable +12V power supply, which is used to power the rest of the battery charging circuitry. This circuitry is shown in Figure 15. This schematic was designed using the Digi-Key SchemeIt software.

The NPN BJT Q_1 and the equivalent resistance of R_3 and R_4 set the maximum charging current to approximately 100mA, based on the component values. When the node at the cathode of the red LED is greater than or equal to 8.3V, the battery will not charge and the charging current will be dumped down the reverse biased Zener diode tree to ground. This is visualized by the red LED turning off and the green LED turning on. The sum of the reverse bias breakdown voltage of diodes D_1, D_2, and the forward bias voltage drop of D_3 is approximately 8.3V. When the node is below 8.3V, then the charging current flows through D_4 and into the battery. This is again visualized, but now by the red LED turning on and the green LED turning off. The charging current is limited to approximately 35mA to protect the battery. As the voltage of the battery increases, the luminous intensity of the red LED decreases and the green LED increases.

Zener diodes, like regular diodes, conduct current from anode to cathode. However, when the voltage drop across a Zener diode is greater than or equal to its Zener voltage, it enters breakdown, which allows it to conduct current from cathode to anode. The cathode of diode D_1 from Figure 15 ranges anywhere from -0.7V in the short circuit condition to approximately 8.3V, when the battery is fully charged. The base-to-emitter voltage drop, V_{BE}, is assumed to be equal to the voltage drop of a silicon pn junction, which is approximately 0.7V. This assumption is standard and is valid in this application. The true value of V_{BE} for different operating points can be found in the datasheet. With this assumption made, the voltage at the base of Q_2, and therefore the anode of D_3, is at approximately 0.7V. The series diode branch was designed for a combined Zener voltage of approximately 8.3V,

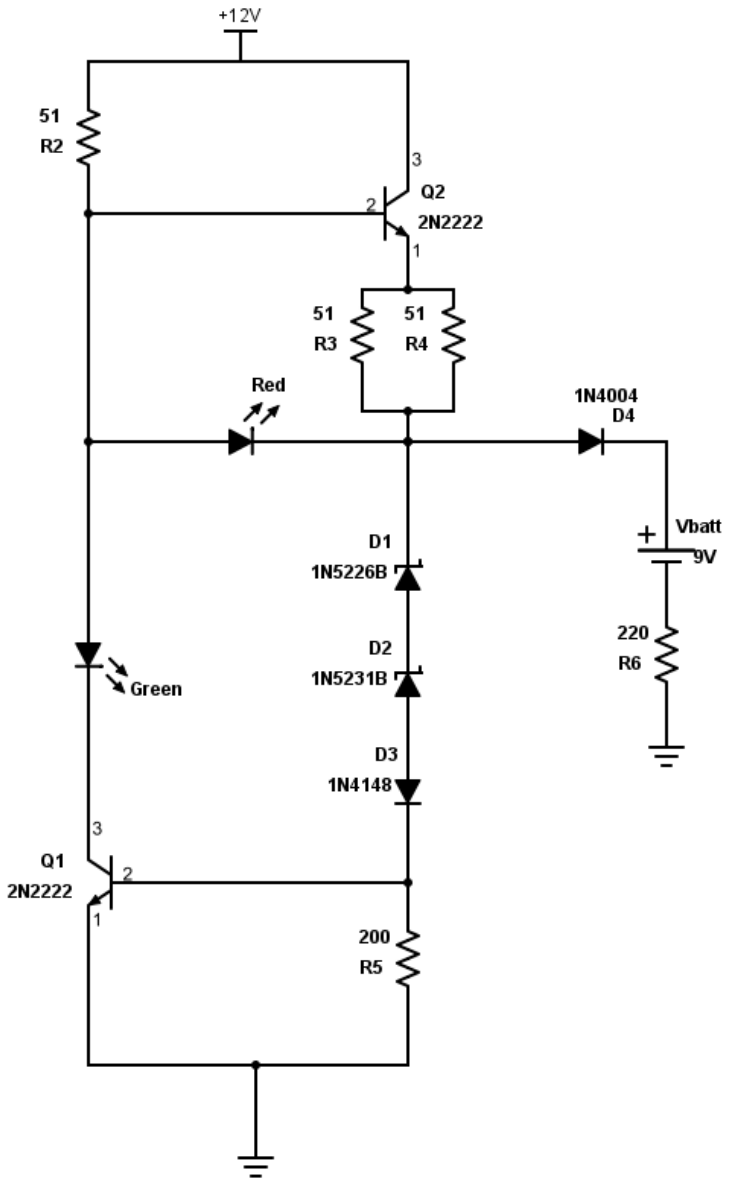

Figure 15: 9V NiCd battery charger

which allows the branch to conduct when the battery is charged. In short, the combined Zener voltage is equivalent to the desired final charge voltage of the battery. The fully connected Receive module schematic is shown in Appendix A.

3.3.2 Power Receiving Construction and Results

The hardware construction involved taking measurements at various points in the analog circuitry to determine whether or not the system would be successful, then performing overall testing. This resulted in multiple iterations of the circuitry, including tuning of component values and circuit layout.

The biggest construction problem that was only somewhat accounted for in the design was the series diode chain reverse breakdown voltage. The initial design of the circuit did not include the 1N4148 and only used Zener diodes. However, the battery was found to only charge up to approximately 7.9V, which is significantly below the nominal 8.4V voltage of 9V NiCd batteries. There were no Zener diodes available with 0.4V Zener voltages, so a 1N4148 was used instead.

The resistor R_6 was added as a current limiting resistor after initial testing. Resistors R_3 and R_4 are used to set the charge current to approximately 100mA. However, this caused too much current to flow through the red LED. Putting the current limiting resistor in series with the battery reduced the current flowing through the LED, but kept the circuit biasing the same.

The testing of the circuit showed just under 12V at the input to the LM7812 12V linear drop out voltage regulator. To measure the charging current, an ammeter was placed in series with D_4 and R_6. The current was measured to be approximately 34.5mA, which was within the specifications outlined in the contract.

4 Wireless Data Transmission

As noted in Section 3.1, power transmission across inductive coils can also be interpreted as data, so long as a standard for interpretation is in place. In the Qi standard, communication takes place using backscatter modulation. There are other common forms of wireless inductive data transmission. One such form is on-off keying, where a sinusoidal carrier signal's presence is measured over a period of time. If the sinusoid is present on the receiving end for a designated amount of time, then the bit is considered a logic one. Otherwise, it is considered a logic zero.

Another form of communication is through phase jitter modulation (PJM). Phase jitter refers to the small offset that makes an oscillatory signal no longer perfectly periodic. An example of phase jitter in the time domain is shown in Figure 16.

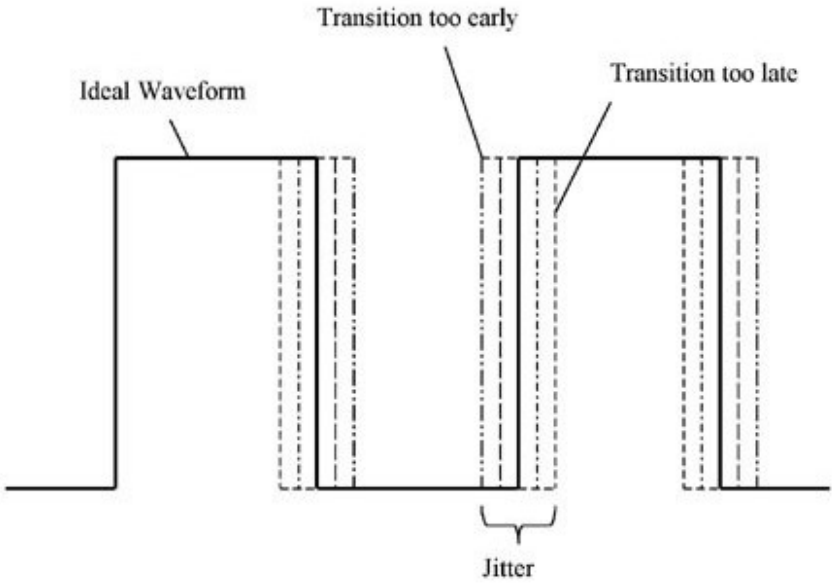

Figure 16: Example of phase jitter in time domain [5]

In PJM, the receiver will purposely introduce jitter into the oscillatory carrier signal transmitted. This signal is then typically sent back to the transmitter, which takes the modulated return signal and compares it against the pure carrier signal. Through various standards, communication between two otherwise unassociated devices can be performed. A common use of PJM is in Near Field Communication (NFC).

4.1 Near Field Communication Applications

NFC is a subset of the Radio Frequency Identification (RFID) protocol that has seen increasing popularity in the smartphone industry over the last decade. In the NFC standard, a device known as the "interrogator" transmits a signal operating at approximately 13.56MHz, per the ISO/IEC 18000-3 standard [6]. If the interrogator is within approximately 4cm of the receiver, referred to as the "tag," communication can start.

The tag is a passive device, meaning that it does not actively power itself. Instead, the tag is powered from the electromagnetic signal transmitted by the interrogator. One can infer that the embedded microcontroller that operates the PJM inside the tag runs code that is stored in a section of non-volatile memory. The interrogator initializes communication with the tag and sends the tag commands. If the tag receives a valid command, it follows with a response.

To be NFC compliant, the interrogator must have full duplex functionality, meaning that it can both transmit and receive data simultaneously. The tag must have half duplex functionality, meaning that it can transmit or receive data, but not at the same time.

The communication channel between the interrogator and the tag is closed if the interrogator chooses to close communications, or if the two devices are physically separated by more

than the standard 4cm.

4.1.1 Application Data Transferal

Numerous applications on the Android Play Store, for example, offer NFC connectivity between two phones. By making an NFC connection, information from one phone, such as contact data, can be transferred to the other [7].

Passive NFC tags can also be programmed using phone applications. These tags can store commands to tell the device once the communication channel is opened between the two devices. These commands can include opening a particular application, changing device settings, or uploading pre-defined data to a server. These tags are available to everyday consumers and, like many other scripting services, act to automate everyday tasks.

4.1.2 Monetary Transactions

Another widespread use for NFC technology is in monetary transactions. Transaction applications, such as Apple Pay or Android Pay, are now being included in operating system standard software. These applications work by storing credit card information in the phone. By enabling NFC channels with tags embedded in a credit card reader terminal, this data is collected and used as a payment method. The card whose information was transmitted is charged for the transaction.

NFC payments offer some benefits to standard card swiping. One such benefit is reduction in effectiveness of PIN skimmers, devices that are physically placed over the keypad of a credit card reader terminal. PIN skimmers store the PIN entered and, combined with the card's information stored on the magnetic strip, allows the user to freely commence transactions with the stolen card.

4.2 Near Field Communication Limitations

Like all other forms of technology, there are drawbacks to NFC. Some of these drawbacks are inherent to the communication protocol itself, namely the proximity requirement. NFC requires devices to be no more than 4cm apart, making it an unsatisfactory form of communication when attempting to transmit data over higher distances. Other wireless communication protocols, such as Bluetooth communication or serial copying over Wi-Fi are required in these kinds of instances.

With the increase of NFC payment methods, sensitive data must be encrypted to prevent attacks from potential hackers. "Eavesdropping" is the act of picking up the NFC signal containing the sensitive information [8]. Avoiding these security risks can be done in multiple ways. One such way is through standard data encryption methods. Another exists inherently in the communication protocol, which is the distance between communicating devices. With a 4cm separation distance, it is physically disadvantageous for a potential hacker to collect the data.

Another form of NFC hacking is an NFC Interception Attack. This is analogous to the PIN skimmer, in that the hacker places a middleman device between the NFC transmitter and the receiver, which can store the information sent by the transmission source, as well as alter the data being sent to the terminal device. These attacks can be prevented by using what is called an "active-passive pairing," which means that only one device can transmit data and the other can only receive data. An inherent limitation to this system is a loss of a confirmation of data transaction, such as a checksum.

5 Conclusion

While wireless power and data transmission has been used in small-scale systems for a number of years, it has only recently been seen in more "everyday consumer" settings. As higher efficiencies are achieved with inductive coupling, transmission distances will see a steady increase. Applications such as wireless battery charging and data transmission through the NFC protocol only begin to scratch the surface of the potential of the technology.

References

[1] Anonymous, "Mutual inductance." web.mit.edu/viz/EM/visualizations/coursenotes/modules/guide11.pdf.

[2] "Wireless electricity transmission - how it works." https://www.wirelesspowerconsortium.com/technology/how-it-works.html.

[3] *System Description - Wireless Power Transfer*, 1.1.2 ed., 2013.

[4] A. Sedra and K. Smith, *Microelectronic Circuits*, ch. 17, pp. 1342–1345. Oxford University Press, Inc, sixth ed., 2009.

[5] N. Roberts, "Phase noise and jitter – a primer for digital designers." http://www.eetimes.com/document.asp?doc_id=1277196, 2003.

[6] Anynomous, "Near field communication technology standards." http://www.nearfieldcommunication.org/technology.html.

[7] Google, "Sharing files with nfc." http://developer.android.com/training/beam-files/index.html.

[8] Anynomous, "Security concerns with nfc technology." http://www.nearfieldcommunication.org/nfc-security.html.

[9] Anonymous, "Simple ni-cd charger." simple-electronics.com/2011/10/simple-ni-cd-charger-automatic.html.

[10] W. Storr, "The wien bridge oscillator." electronics-tutorials.ws/oscillator/wien_bridge.html.

A Schematics

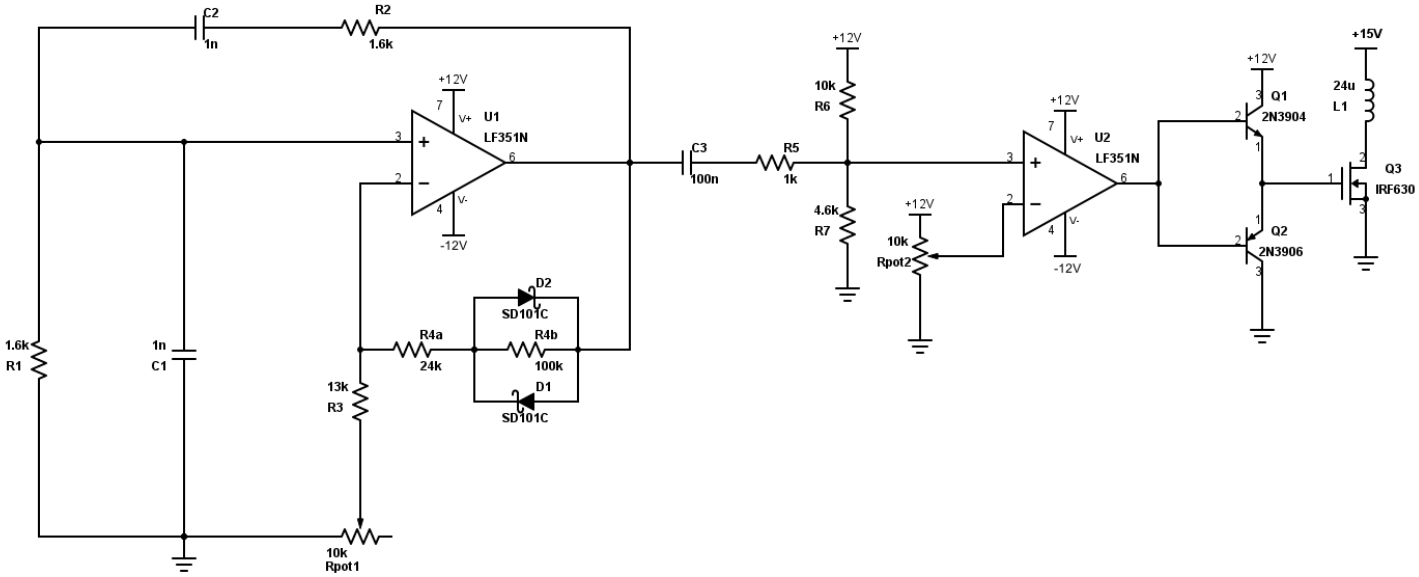

Figure 17: Final transmitter schematic

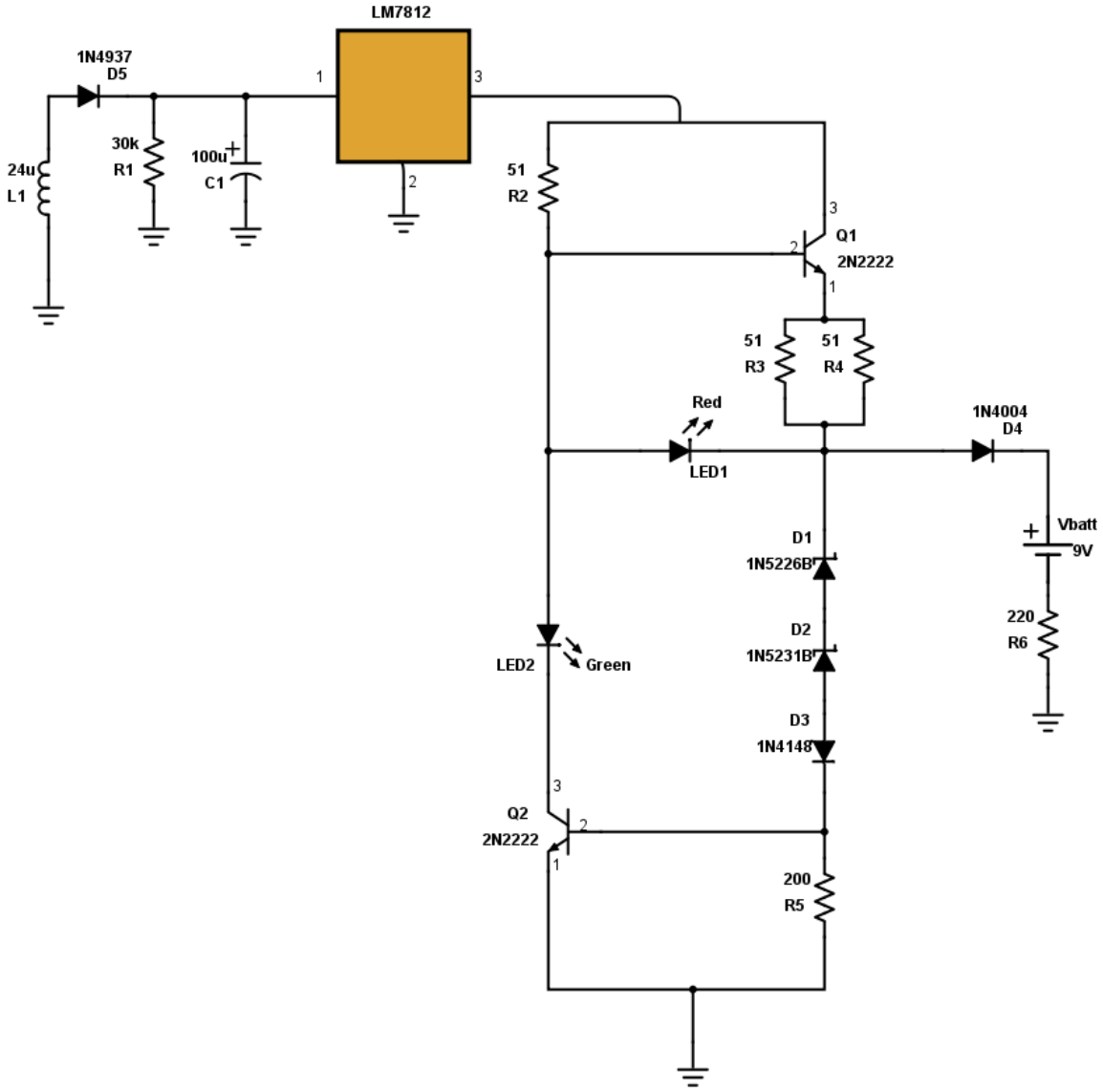

Figure 18: Final receiver schematic

Biography

Seth Raymond was born in Bangor, Maine on Feburary 28, 1994. He was raised in Prospect, Maine and graduated from Bucksport High School in 2012. Seth graduated from the University of Maine in May 2016 with a Bachelor of Science in Electrical and Computer Engineering, along with a minor in Mathematics. He is a member of the IEEE honors society, Eta Kappa Nu, where he served as the Vice President for the 2015-2016 academic year in the Delta Kappa Chapter. He has received numerous scholarships in his undergraduate career, including the University of Maine Pulp and Paper Foundation Scholarship and the Science Mathematics And Research for Transformation (SMART) Scholarship.

Upon completion of his undergraduate degree, Seth began work at the Naval Surface Warfare Center in Dahlgren, Virginia as a civilian engineer in completion of the service requirement specified in the SMART Scholarship.